Molecular Pharmacology Fast Forward. Published on July 21, 2005 as doi: 10.1124/mol.104.008367
This article has been copyedited and formatted. The final version may differ from this version.

MOL 8367

Mechanisms for the Inhibition of DNA Methyltransferases by Tea Catechins and Bioflavonoids

Won Jun Lee, Joong-Youn Shim and Bao Ting Zhu[1]

Department of Basic Pharmaceutical Sciences, College of Pharmacy, University of South Carolina, Columbia, SC 29208, USA (*W.J.L.*, *B.T.Z.*)

and

J. L. Chambers Biomedical/Biotechnology Research Institute, North Carolina Central University, Durham, NC 27707 (*J.-Y.S.*)

Molecular Pharmacology Fast Forward. Published on July 21, 2005 as DOI: 10.1124/mol.104.008367
This article has not been copyedited and formatted. The final version may differ from this version.

MOL 8367

Running title*:* Modulation of DNA methylation by dietary polyphenols

Corresponding author: Bao Ting Zhu, Ph.D. Frank and Josie P. Fletcher Professor of Pharmacology and an American Cancer Society Research Scholar, and to whom requests for reprints should be addressed at the Department of Basic Pharmaceutical Sciences, College of Pharmacy, University of South Carolina, Room 617 of Coker Life Sciences Building, 700 Sumter Street, Columbia, SC 29208 (USA).
PHONE: 803-777-4802; FAX: 803-777-8356; E-MAIL: BTZhu@cop.sc.edu

Number of text pages : 34

Number of tables : 2

Number of figures : 10

Number of references : 39

Number of words in abstract : 229

Number of words in introduction : 458

Number of words in discussion : 1567

Molecular Pharmacology Fast Forward. Published on July 21, 2005 as DOI: 10.1124/mol.104.008367
This article has not been copyedited and formatted. The final version may differ from this version.

ABSTRACT

In the present investigation, we studied the modulating effects of several tea catechins and bioflavonoids on DNA methylation catalyzed by prokaryotic *SssI* DNA methyltransferase (DNMT) and human DNMT1. We found that each of the tea polyphenols (catechin, epicatechin, and [-]-epigallocatechin-3-*O*-gallate [EGCG]) and bioflavonoids (quercetin, fisetin, and myricetin) inhibited *Sss*I DNMT- and DNMT1-mediated DNA methylation in a concentration-dependent manner. The IC_{50} values for catechin, epicatechin, and various flavonoids ranged from 1.0 – 8.4 μM, but EGCG was a more potent inhibitor, with IC_{50} values at 0.21 – 0.47 μM. When epicatechin was used as a model inhibitor, kinetic analyses showed that the mechanism by which this catechol-containing dietary polyphenol inhibited enzymatic DNA methylation *in vitro* largely through increased formation of *S*-adenosyl-*L*-homocysteine (a potent noncompetitive inhibitor of DNMTs) during the catechol-*O*-methyltransferase-mediated *O*-methylation of this dietary catechol. In comparison, the strong inhibitory effect of EGCG on DNMT-mediated DNA methylation was independent of its own methylation, and it was largely due to its direct inhibition of the DNMTs. This inhibition is strongly enhanced by Mg^{2+}. Computational modeling studies showed that the gallic acid moiety of EGCG plays a crucial role in its high-affinity, direct inhibitory interaction with the catalytic site of the human DNMT1, and its binding with the enzyme is stabilized by Mg^{2+}. The modeling data on the precise molecular mode of EGCG's inhibitory interaction with human DNMT1 agrees perfectly with our experimental finding.

Molecular Pharmacology Fast Forward. Published on July 21, 2005 as DOI: 10.1124/mol.104.008367
This article has not been copyedited and formatted. The final version may differ from this version.

INTRODUCTION

DNA methylation at the C5-position of cytosine within the CpG dinucleotides represents an important mechanism for epigenetic control of gene expression and the maintenance of genome integrity. While DNA hypermethylation is associated with inactivation of genes, global genomic hypomethylation is often associated with the induction of chromosomal instability (Chen et al., 1998). A number of recent studies have suggested that bioactive food components, including both essential and nonessential nutrients, can modify DNA methylation patterns in complex ways. For instance, consumption of a methyl-deficient diet led to hypomethylation of specific CpG sites within several oncogenes (such as c-myc, c-fos, and c-H-ras), resulting in elevated levels of mRNA for these genes (Wainfan and Poirier, 1992). A recent study showed that tea catechins are effective inhibitors of human DNA methyltransferase (DNMT)-mediated DNA methylation *in vitro* and in cultured cancer cells (Fang et al., 2003).

DNA methylation is catalyzed by specific DNMTs[2]. Multiple DNMTs are known to be present in humans, animals, and microorganisms, and they have varying degrees of specificity towards unmethylated and hemi-methylated DNA substrates (Bestor and Ingram, 1983). *S*-Adenosyl-*L*-methionine (SAM) is the methyl donor in the DNMT-mediated DNA methylation, as in many other enzymatic methylation reactions (such as the catechol-*O*-methyltransferase [COMT]-mediated *O*-methylation of various catechol substrates), resulting in the formation of *S*-adenosyl-*L*-homocysteine (SAH) after donating its methyl group to the DNA substrate.

It is known that various catechol-containing dietary polyphenols are excellent substrates for the COMT-mediated *O*-methylation (Zhu et al., 1996; Zhu and Liehr, 1996; Zhu et al., 2000; Zhu et al., 2001). The COMT-mediated methylation of large amounts of dietary catechols would not only reduce the cellular pools of SAM, but it would also form an equimolar amount of SAH (demethylated SAM), a feedback inhibitor of various SAM-dependent methylation reactions. Hence, it is hypothesized that the facile metabolic *O*-methylation of various catechol-containing

Molecular Pharmacology Fast Forward. Published on July 21, 2005 as DOI: 10.1124/mol.104.008367
This article has not been copyedited and formatted. The final version may differ from this version.

dietary polyphenols may be an important cumulative factor that affects the rate of DNA methylation (depicted in **Fig. 1A**), and this possibility was investigated in the present study. Specifically, we studied the mechanism of inhibition of enzymatic DNA methylation by catechol-containing polyphenols from two common classes, namely, tea catechins (catechin, epicatechin, and EGCG) and bioflavonoids (quercetin, fisetin, and myricetin) (structures shown in **Fig. 1B**). The recombinant prokaryotic *Sss*I DNMT and human DNMT1 (a dominant form of the DNMTs in humans) were used in the present study as model enzymes for the following two reasons. First, the *Sss*I DNMT is functionally similar to the human DNMT3A and DNMT3B, and methylates both unmethylated and hemi-methylated DNA substrates with almost equal efficiency (Okano et al., 1998), whereas the human DNMT1 preferentially methylates hemi-methylated DNA over unmethylated DNA. Second, both of the enzymes are commercially available as selectively-expressed proteins, which provide a stable source of enzymes needed for our study.

Molecular Pharmacology Fast Forward. Published on July 21, 2005 as DOI: 10.1124/mol.104.008367
This article has not been copyedited and formatted. The final version may differ from this version.

MATERIALS AND METHODS

Chemicals

Catechin, epicatechin, EGCG, quercetin, fisetin, myricetin, SAM, SAH, and porcine liver COMT (affinity column-purified, 1396 units/mg of protein) were purchased from the Sigma Chemical Co. (St. Louis, MO). The synthetic double-stranded poly(dG-dC)·poly(dG-dC) and poly(dI-dC)·poly(dI-dC) were obtained from Amersham Pharmacia Biotech (Piscataway, NJ). The average lengths of the poly(dG-dC)·poly(dG-dC) and poly(dI-dC)·poly(dI-dC) were 920 and 5469 base pairs, respectively. The prokaryotic *Sss*I DNMT and the human DNMT1 were obtained from the New England Biolabs (Beverly, MA). According to the supplier, the *Sss*I DNMT was isolated from a strain of *E. coli* transfected with the *Sss*I DNMT gene from the *Spiroplasma sp.* strain MQ1 (Renbaum et al., 1990), and it was stored at -20ºC (at 200 unit/50 μl) in a buffer containing 10 mM Tris-HCl (pH 7.4), 0.1 mM ethylenediaminetetraacetic acid (EDTA), 1 mM dithiothreitol, 200 μg/ml bovine serum albumin, and 50% glycerol. DNMT1 was stored in a buffer containing 50 mM Tris-HCl (pH 7.5), 1 mM EDTA, 1 mM dithiothreitol, 7 μg/ml phenylmethanesulfonyl fluoride (PMSF), 50% glycerol, and the protease inhibitor cocktail. The cocktail contained 4-(2-aminoethyl)benzenesulfonyl fluoride, pepstatin A, E64, bestatin, leupeptin, and aprotinin. [Methyl-^{3}H]SAM (specific activity of 11.2-13.5 Ci/mmol) was purchased from New England Nuclear Research Products (Boston, MA). The ScintiVerse BD scintillation cocktail was obtained from Fisher Scientific (Pittsburgh, PA).

Assay of enzymatic DNA methylation *in vitro*

The following reaction mixtures were freshly prepared on ice immediately prior to carrying out the *in vitro* DNA methylation reaction. The poly(dG-dC)·poly(dG-dC) and poly(dI-dC)·poly(dI-dC) substrates were diluted in the TE buffer (containing 10 mM Tris-HCl and 1 mM EDTA, pH

Molecular Pharmacology Fast Forward. Published on July 21, 2005 as DOI: 10.1124/mol.104.008367
This article has not been copyedited and formatted. The final version may differ from this version.

7.6) to desired stock concentrations, usually at 250 μM of the CpG methylation sites. Note that 1 mole of the double-stranded dG-dC:dG-dC or dI-dC:dI-dC dinucleotides was considered to contain 2 moles of the CpG methylation sites. The stock solutions of *Sss*I DNMT and DNMT1 were further diluted in water usually to a concentration of 1 unit/5 μl. The methyl donor SAM (containing ~0.5 μCi [methyl-^{3}H]SAM) was dissolved in 0.8 mM HEPES at desired stock concentrations depending on the experiments. As recommended by the supplier of the DNMTs, the reaction buffer for *Sss*I DNMT consisted of 50 mM NaCl, 10 mM Tris-HCl, 10 mM $MgCl_2$, 1.0 mM dithiothreitol (pH 7.9), and the reaction buffer for DNMT1 consisted of 50 mM Tris-HCl, 1 mM EDTA, 1 mM dithiothreitol, and 5% glycerol (pH 7.8).

The above freshly-prepared solutions were then added in a sequential order to a 1.5-ml microcentrifuge tube on ice: 5 μl of the reaction buffer, 5 μl of the synthetic DNA substrate, 5 μl of the enzyme, 5 μl water, and 5 μl SAM (mixed with [methyl-^{3}H]SAM). Notably, in some of the experiments designed to study the effects of dietary chemicals in the presence of COMT, the 5-μl volume of water was replaced with 2.5 μl of COMT (at 2 units/2.5 μl for *Sss*I DNMT and 4 units/2.5 μl for DNMT1) and 2.5 μl of a dietary chemical (added separately to the reaction mixture). As such, the final reaction mixture usually contained 0.125-10 μM of the CpG methylation sites, 1.25-20 μM of SAM (containing ~0.5 μCi [methyl-^{3}H]SAM), and 0.25-4 units of the enzyme in a final volume of 25 μl. Considering that Mg^{2+} ion is a necessary cofactor for the activity of COMT, $MgCl_2$ (at a final concentration of 2 mM) was added into the DNMT1-mediated reaction tube because the corresponding reaction buffer provided by the supplier did not contain $MgCl_2$. The incubations were carried out at 37ºC for varying lengths of time, and the reactions were arrested by immediately placing the tubes on ice, followed by addition of 145 μl ice-cold 0.9% sodium chloride and 100 μl salmon testes DNA (at 1 mg/ml in the TE buffer). To precipitate the DNA, 30 μl of 3 M sodium acetate and 900 μl ice-cold ethanol (95%) were added, and the samples were placed in a -80°C freezer for 2 hrs. After centrifugation at ~10,000 *g* for 10 min, 100 μl of the heat-deactivated flour (suspended at 40 mg/ml in double-distilled water) was added to each tube, followed by

Molecular Pharmacology Fast Forward. Published on July 21, 2005 as DOI: 10.1124/mol.104.008367
This article has not been copyedited and formatted. The final version may differ from this version.

centrifugation at ~10,000 *g* for 5 min. This step was designed to firmly secure the precipitated DNA pellet (including the methylated poly[dG-dC]·poly[dG-dC] or poly[dI-dC]·poly[dI-dC]) at the bottom of the microcentrifuge tubes which would prevent the pellet from being partially washed away during the following washing steps. Notably, our comparison of various measurements showed that the addition of the flour made the intra-assay as well as inter-assay variations much smaller when compared to the parallel assays without flour. The pellets were then gently washed 3 times with 70% ethanol, and each wash was followed by centrifugation for 3 min at 10,000 *g*. The pellets (containing DNA and flour) were then resuspended in 30 μl of 100% ethanol and 1 ml of TE buffer (pH 7.6). Each vial was sonicated for ~10 min and vortexed thoroughly to assure adequate resuspension of the pellet, and then the content was transferred to a scintillation vial (containing 4 ml of ScintiVerse BD) for measurement of ^{3}H-radioactivity with a liquid scintillation counter (Packard Tri-CARB 2900 TR; Downers Grove, IL). Corresponding blank values obtained from incubations in the absence of the DNA substrate were also determined in each individual assay and subtracted. Since the same amount (1 unit) of the *Sss*I DNMT and DNMT1 was used in most of the assays (unless otherwise indicated), the rate of DNA methylation, mediated by *Sss*I DNMT or human DNMT1, was usually expressed as "*pmol of methylated sites formed per minute*" (abbreviated as "*pmol/min*"). The kinetic parameters (K_M and V_{MAX} values) were calculated manually according to the Eadie-Hofstee plots (*V* versus *V*/[*S*]).

Determination of the methylation status of RARβ gene in cultured cancer cells

Two human breast cancer cell lines (MCF-7 and MDA-MB-231) were used in this study and they were obtained from the American Type Culture Collection (Manassas, VA). The culture of these cells was described in detail in our recent study (Liu and Zhu, 2004). The MDA-MB-231 and MCF-7 cells were treated with 0, 0.2, 1, 5, 25, or 50 μM of EGCG for 3 or 6 days, respectively, depending on the rate of cell growth. Cells were then harvested for DNA extraction by using the DNeasy tissue kit (Qiagen, Valencia, CA). The extracted DNA (1 μg) was modified by EZ DNA

Molecular Pharmacology Fast Forward. Published on July 21, 2005 as DOI: 10.1124/mol.104.008367
This article has not been copyedited and formatted. The final version may differ from this version.

methylation kit (Zymo Research, Orange, CA) under conditions specified by the supplier. All unmethylated cytosines were converted to uracils, whereas 5-methylcytosines remained unaltered. The methylation status of the RARβ genes was determined by using a nested two-stage PCR approach (Palmisano et al., 2000). Sodium bisulfite-modified DNAs were first subjected to the stage-I PCR to amplify the 425-bp fragments of the RARβ gene (see **Table 1**). The stage-I PCR products include a portion of the CpG-rich promoter region of the gene. The primers (from Invitrogen Life Technologies, Frederick, MD) for the stage-I PCR recognized the bisulfite-modified template but did not discriminate between methylated and unmethylated alleles. The stage-I PCR products were diluted 50-1000 times, and 2.5 μl of the diluted PCR products was subjected to a stage-II PCR with primers specifically designed for the methylated or unmethylated template. The sequences of the primers, annealing temperatures, and product sizes used in the stage-I and stage-II PCR amplifications of the RARβ gene are summarized in **Table 1**. HotStarTaq DNA polymerase (Qiagen, Valencia, CA) in a 25-μl reaction volume was used in all PCRs. The conditions for the stage-I PCR were as follows: 95°C for 15 min, then denaturing at 95°C for 45 s, annealing at 53°C for 1 min, extension at 72°C for 1 min for 40 cycles followed by a final extension at 72°C for 10 min. Conditions for the stage-II PCR included 95°C for 15 min, then denaturing at 95°C for 30 s, annealing at 62°C at 30 s, extension at 72°C for 30 s for 18-30 cycles and a final 10-min extension step at 72°C. The number of cycles and the PCR conditions were optimized so that the amplified signal was still on the linear portion of the amplification curve. Controls (without DNA) were included for each set of PCRs. Amplified PCR products were subjected to electrophoresis using 2% agarose gels, stained with ethidium bromide, directly visualized with ultraviolet transillumination, and photographed. The integrated optical density (IOD) of each band was quantified by densitometry. The relative levels of methylated and unmethylated PCR products were normalized against the PCR products obtained by using another set of primers specifically designed to amplify the regions which served as internal standard for the stage-I PCR products (depicted in **Table 1**). The primers for the internal standard would not discriminate between methylated and unmethylated

Molecular Pharmacology Fast Forward. Published on July 21, 2005 as DOI: 10.1124/mol.104.008367
This article has not been copyedited and formatted. The final version may differ from this version.

alleles. All PCR amplifications were carried out using a PTC-100 thermal cycler (MJ Research, Waltham, MA).

Computational modeling of the binding of EGCG to human DNMT1

Energy minimizations, molecular dynamics simulations, and molecular docking experiments were performed on a Silicon Graphics Origin-350 workstation using the consistent valence force field (CVFF) (Dauber-Osguthorpe et al., 1998) implemented in the *InsightII* program (Version 2000, Accelrys Inc. San Diego, CA). The cell multipole method (Ding et al., 1992) with a distance-dependent dielectric constant ($\varepsilon = \varepsilon_0 r$, with $\varepsilon_0 = 4.0$) was used for summation of non-bonding interactions. For energy minimizations, the steepest descent method was employed first to a 100 kcal/molÅ energy gradient and followed by the Polak and Ribiere conjugate gradients method (Press et al., 1993) until the final convergence criterion reached the 0.01-kcal/molÅ energy gradient.

Homology model of human DNMT1. The primary sequences of human DNMT1 (GI: 4503351) and *Hha*I methylase (GI: 127455) were obtained from the NCBI database. Based on a recent suggestion that the Class I DNMTs share similar catalytic core regions (Schubert et al., 2003), a homology model of the human DNMT1 was thus constructed by using *Hha*I methylase (PDB code: 5MHT) as a template after multiple sequence alignments with *CLUSTAL W* (Higgins et al., 1996). SAM was included in this model because this cofactor is required for maintaining the structural fold and the normal catalytic function of the enzyme (Martin and McMillan, 2002). The variable loop regions were initially constructed using the random loop search method. The whole enzyme structure was then subjected to a combination of constrained molecular dynamics and simulated annealing (starting at a temperature of 1500 K and then cooling down to a temperature of 300 K) procedures (Fiser et al., 2000), during which the conserved β-sheet and α-helical structures that form the catalytic crevice and bind the DNA double helix were held in a fixed configuration, while the carboxylate moiety of SAM was constrained to Cys1147 and Gly1149 of the enzyme with

Molecular Pharmacology Fast Forward. Published on July 21, 2005 as DOI: 10.1124/mol.104.008367
This article has not been copyedited and formatted. The final version may differ from this version.

hydrogen bonds. A set of 25 conformations collected from this procedure were then subjected to a sequence of energy minimizations: (**i**) minimization with the DNA double helix fixed and the hydrogen bonds constrained; (**ii**) minimization with the DNA double helix freed; and finally, (**iii**) minimization without any constraint. Selected among the lowest energy conformations, the final structure was validated using the *Profiles-3D* program (Bowie et al., 1991), and was used as template for the docking of EGCG molecule.

Molecular docking of EGCG. After the DNA double helical structure was removed from the DNMT1's structural model, an energy-minimized EGCG structure generated by the *Builder* module in *InsightII* program was manually positioned within the catalytic core region between SAM and the catalytic site where the target cytosine base is positioned in a flipped-out position. In this study, the binding pocket was defined to include all the residues within 16 Å reach of the EGCG molecule, and then a combination of Monte Carlo (MC) and molecular dynamics simulation procedures were performed to explore the binding conformations of EGCG using the *Affinity* module of the *InsightII* program. During this procedure, EGCG and the side chains of the amino acid residues within the defined binding site were allowed to rotate freely. Among 100 conformations obtained from MC sampling, the most likely binding conformation was determined, which would have the lowest energy among the minimized structures and would have maximal hydrogen bonding interaction.

Binding energy analysis. The binding energy calculations were performed using the semiempirical PM3 method (Stewart, 1989) for a model system comprising EGCG, SAM and a group of key catalytic site residues (Lys1482, Cys1225, Glu1265, Asn1266, Val1267, Arg1311, and Asn1577) within 3 Å reach of the docked EGCG molecule. During the calculation, atoms in the backbone-heavy amino acids were fixed in positions. Furthermore, to explore the impact of Mg^{2+} on the inhibitory potency of EGCG, the binding energy (ΔE_{bind}) was calculated after Mg^{2+}, and water molecules were appropriately introduced to form a plausible Mg^{2+}-coordinated EGCG complex in the catalytic site. It was assumed that Mg^{2+} would be in a monodentate state, for this coordination

Molecular Pharmacology Fast Forward. Published on July 21, 2005 as DOI: 10.1124/mol.104.008367
This article has not been copyedited and formatted. The final version may differ from this version.

mode likely is predominant based on previous X-ray structural studies of several other Mg^{2+}-containing proteins (Dudev and Lim, 2003). Accordingly, water molecules were also included in our proposed computational model to satisfy the preferred octahedral coordination geometry of Mg^{2+} (Dudev and Lim, 2003).

Molecular Pharmacology Fast Forward. Published on July 21, 2005 as DOI: 10.1124/mol.104.008367
This article has not been copyedited and formatted. The final version may differ from this version.

RESULTS

Inhibition of DNMT-mediated DNA methylation by tea polyphenols and bioflavonoids

DNA methylation conditions. Before we studied the effects of various dietary chemicals on DNA methylation, we first optimized the reaction conditions for the *in vitro* DNA methylation by determining the effects of different incubation times and the effects of different concentrations of the enzyme (prokaryotic *Sss*I DNMT or human DNMT1), of the methyl donor SAM, and of the synthetic DNA substrates. Based on these measurements, a common reaction condition was devised for both *Sss*I DNMT- and DNMT1-mediated DNA methylation reactions, which included an incubation time of 30 min, an enzyme concentration of 1 unit/25 μl, a SAM concentration of 5 μM, and the substrate concentrations from 0.1-5 μM (*data not shown*). Notably, in some of the experiments designed to determine the modulating effects of the catechol-containing dietary chemicals on the rate of DNA methylation *in vitro*, COMT was also added to the reaction mixture, in addition to the dietary chemical. The concentration of porcine liver COMT used in the present study was 2 units/25 μl for *Sss*I DNMT and 4 units/25 μl for DNMT1. Our measurements showed that COMT at these concentrations provided physiologically-relevant rates of methylation of representative catechol substrates assayed (such as catechol estrogens and tea catechins) (*data not shown*).

Inhibition by tea catechins. Catechin and epicatechin inhibited the *Sss*I DNMT-mediated DNA methylation in a concentration-dependent manner (**Fig. 2A, 2B**). The IC_{50} values of catechin and epicatechin for inhibition of DNA methylation were 6.5 and 8.1 μM, respectively, and the maximal inhibition at the highest concentration (20 μM) of these two inhibitors were ~60% in the presence of COMT. In comparison, EGCG exerted a more potent and efficacious inhibition of the *Sss*I DNMT-mediated DNA methylation (**Fig. 2C**). The apparent IC_{50} value of EGCG was ~0.21 μM, which was ~30 times more potent than catechin and ~40 times more potent than epicatechin, and a nearly complete inhibition was seen at 5 μM of EGCG. The strong inhibition of DNA

Molecular Pharmacology Fast Forward. Published on July 21, 2005 as DOI: 10.1124/mol.104.008367
This article has not been copyedited and formatted. The final version may differ from this version.

methylation by EGCG was repeated over 3 times, and consistent results were obtained. It should be noted that when COMT was not added to the reaction system, catechin or epicatechin alone at the 20-μM concentration also exerted varying degrees of direct inhibition of *Sss*I DNMT-mediated DNA methylation (**Fig. 2A, 2B**). In contrast, EGCG had a strong direct inhibition of DNA methylation (**Fig. 2C**). Although the potency of EGCG's direct inhibition was lower than that its overall inhibition when COMT was present, the efficacy of its direct inhibition was comparable to its overall inhibition (**Fig. 2C**). Taken together, these results showed that while the metabolic *O*-methylation of catechin and epicatechin markedly increased their overall activity for inhibition of *SssI* DNMT-mediated DNA methylation, but the methylation of EGCG did not appear to significantly increase its inhibitory efficacy on DNA methylation.

When human DNMT1 was tested as the enzyme, the inhibitory effect of catechin, epicatechin, and EGCG on enzymatic DNA methylation was similar to their inhibition of *Sss*I DNMT-mediated DNA methylation (**Fig. 2D, 2E, 2F**). The apparent IC_{50} values of catechin and epicatechin for inhibition of DNMT1-mediated DNA methylation were 4.6 and 8.4 μM, respectively, and their maximal inhibition at the highest 20-μM inhibitor concentration was ~80%. In comparison, EGCG (IC_{50} = 0.47 μM) exerted a 10 to 20 times more potent inhibition of the human DNMT1 than did catechin and epicatechin. Notably, in the absence of COMT, catechin or epicatechin alone at the 20-μM concentration also exerted certain degrees of direct inhibition of the DNMT1-mediated DNA methylation (**Fig. 2D, 2E**). In comparison, EGCG had a stronger direct inhibition of DNA methylation, which had the similar potency and efficacy as in the presence of COMT (**Fig. 2F**).

Inhibition by bioflavonoids. Several common catechol-containing bioflavonoids (quercetin, fisetin, and myricetin) were also tested for their activity in inhibiting DNA methylation. Each of the tested bioflavonoids inhibited *Sss*I DNMT-mediated DNA methylation in a concentration-dependent manner (**Fig. 3A**). The IC_{50} values of quercetin, fisetin, and myricetin for inhibition of *Sss*I DNMT were 1.6, 1.0, and 0.7 μM, respectively (**Fig. 3A**). Myricetin was slightly

Molecular Pharmacology Fast Forward. Published on July 21, 2005 as DOI: 10.1124/mol.104.008367
This article has not been copyedited and formatted. The final version may differ from this version.

more potent and efficacious than quercetin and fisetin for inhibition of DNA methylation. When COMT was not added to the test system, quercetin or fisetin at the highest concentration tested (20 μM) only had a very weak direct inhibition of *Sss*I DNMT-mediated DNA methylation. In comparison, myricetin at the same concentration had a stronger direct inhibition (~60%) of DNA methylation. This stronger direct inhibition by myricetin likely also determines its higher overall inhibitory efficacy on DNA methylation.

The overall inhibitory effect of quercetin, fisetin, and myricetin on human DNMT1-mediated DNA methylation was similar to their inhibition of *Sss*I DNMT-mediated DNA methylation (**Fig. 3B**). While the direct inhibition by quercetin or fisetin (at the 20-μM concentration) in the absence of COMT was rather weak, myricetin exerted a quite strong direct inhibition. In the presence of COMT, the apparent IC_{50} values of quercetin, fisetin, and myricetin for inhibition of the DNMT1-mediated DNA methylation were 1.6, 3.5, and 1.2 μM, respectively.

Inhibition of the promoter region DNA methylation in cultured cells by EGCG and catechin

A recent study showed that treatment of cultured cells with EGCG affected the methylation status of certain genes in human esophageal squamous cell carcinoma cell lines KYSE 510 and KYSE 150 (Fang et al., 2003). In the present study, we compared the effects of EGCG with catechin on the methylation status of RARβ gene in two human breast cancer cell lines (MCF-7 and MDA-MB-231). It is known that RARβ gene promoter region in MCF-7 and MDA-MB-231 cells was hypermethylated (Sirchia et al., 2000). Morphologically, the MCF-7 and MDA-MB-231 cells treated with EGCG or catechin at concentrations up to 50 μM showed little sign of cytotoxicity (**Fig. 4**). Based on the measurement of the amount of total isolated DNA from each treatment group of the cultured cancer cells, the rate of cell growth was only slightly inhibited (<15%) by EGCG or catechin (at 50 μM) in MDA-MB-231 cells and it was basically not affected in MCF-7 cells by these two tea polyphenols (*data not shown*).

Molecular Pharmacology Fast Forward. Published on July 21, 2005 as DOI: 10.1124/mol.104.008367
This article has not been copyedited and formatted. The final version may differ from this version.

The methylation-specific and unmethylation-specific bands of RARβ gene were both detected in these two human breast cancer cell lines when EGCG was not present. It is of note that the relative density of the methylation- and unmethylation-specific bands of the genes as shown in **Fig. 5** did not represent the real ratios between the methylation and unmethylation bands because the ratios might have been altered following two stages of nested PCR amplification. Following treatment of MCF-7 cells with EGCG at 0, 0.2, 1, 5, 25 and 50 μM for 6 days, the unmethylation-specific bands for the promoter region of the RARβ gene were found to be increased in a dose-dependent manner, while the methylation-specific bands were decreased dose-dependently (**Fig. 5**). In the MDA-MB-231 cells, the change of the methylation status of the RARβ promoter region by EGCG treatment was very similar to that observed in MCF-7 cells (**Fig. 5**). In similar ways, the unmethylation-specific bands for the promoter region of p16 gene were increased in cultured T-47D human breast cancer cells after treatment with 5 or 20 μM EGCG, while the methylation-specific bands were decreased (*data not shwon*). For comparison, we also determined the effects of catechin on the methylation status of the RARβ gene in MCF-7 and MDA-MB-231 cells. The overall change of the methylation status in these cells after treatment with catechin was similar to the treatment with EGCG, but EGCG had a more potent and somewhat stronger inhibitory effect on DNA methylation than did catechin (**Fig. 5**).

Kinetic mechanisms for the inhibition of DNA methylation by tea polyphenols

Epicatechin. Using epicatechin as a representative dietary catechol, we determined the kinetic features of its inhibition of DNMT-mediated DNA methylation. We found that at a relatively low inhibitor concentration (2 μM), epicatechin decreased the V_{MAX} values of the *Sss*I DNMT-mediated DNA methylation, but it also slightly decreased the apparent K_M values. At a higher inhibitor concentration (10 μM), the V_{MAX} values were further decreased in a concentration-dependent manner, but the K_M values were basically not further changed (**Fig. 6A**). This suggests a

Molecular Pharmacology Fast Forward. Published on July 21, 2005 as DOI: 10.1124/mol.104.008367
This article has not been copyedited and formatted. The final version may differ from this version.

predominantly noncompetitive mechanism of inhibition when higher inhibitor concentrations were present. A decrease in the V_{MAX} values was also observed when the human DNMT1-mediated DNA methylation was assayed in the presence of epicatechin (**Fig. 6B**).

To gain a better understanding of the kinetic mechanism(s) for the observed inhibition of DNA methylation by catechol-containing dietary polyphenols, we also determined the effects of SAH on the *Sss*I DNMT- and human DNMT1-mediated DNA methylation. Representative data for the regulation of human DNMT1-mediated DNA methylation by SAH are shown in **Fig. 7**. We found that SAH was a very potent inhibitor of the DNMT1-mediated DNA methylation *in vitro*, and the estimated IC_{50} values for SAH were ~0.34 μM (**Fig. 7A**). Notably, this inhibition by SAH is independent of the DNA substrate concentrations used (*data not shown*). Enzyme kinetic analyses showed that when a fixed concentration of SAM was present, increasing the concentrations of SAH resulted in continuous decreases of the V_{MAX} values of the DNMT1-mediated DNA methylation but the K_M values were essentially not altered (**Fig. 7B**), clearly indicating that SAH was a noncompetitive inhibitor with respect to the formation of the methylated DNA products. This finding is in agreement with earlier studies showing that SAH is essentially a noncompetitive inhibitor of the DNMTs (James et al., 2003).

Taken together all the data we gathered, we came to the conclusion that there are two mechanistic components involved in the inhibition of DNA methylation by some of the catechol-containing dietary polyphenols (such as catechin and epicatechin): one is the direct inhibition of the DNMTs (independent of COMT-mediated methylation), and the other is the indirect inhibition of the enzyme through increased formation of SAH during COMT-mediated methylation of the dietary chemicals.

EGCG. Since our earlier studies showed that EGCG was *O*-methylated by COMT to a much lesser degree than catechin and epicatechin, its strong inhibition activity towards DNA methylation as observed in the present study mostly did not result from its metabolic *O*-methylation and the

Molecular Pharmacology Fast Forward. Published on July 21, 2005 as DOI: 10.1124/mol.104.008367
This article has not been copyedited and formatted. The final version may differ from this version.

subsequent formation of SAH. In agreement with this suggestion, we found that EGCG displayed a similar efficacy for inhibition of DNA methylation in the absence of COMT, whereas this was not the case with catechin and epicatechin (**Fig. 2**). During our search for the possible mechanism(s) for the potent inhibition of DNA methylation by EGCG, we found that while *Sss*I DNMT-mediated DNA methylation was essentially not affected by $MgCl_2$ at up to 10 mM concentrations (the highest concentration tested), the human DNMT1-mediated DNA methylation was inhibited by the presence of $MgCl_2$ in a concentration-dependent manner (**Fig. 8A, 8C**). Most importantly, the inhibition potency (IC_{50} value) of EGCG for human DNMT1-mediated DNA methylation was markedly enhanced by $MgCl_2$ (**Fig. 8D**). In comparison, the inhibition of *Sss*I DNMT-mediated DNA methylation by EGCG was only slightly enhanced by $MgCl_2$ (**Fig. 8B**). Since the presence of equimolar concentrations of Cl^- (from NaCl or KCl) did not show any appreciable effects as observed with $MgCl_2$ (*data not shown*), it was thus believed that the inhibitory effects of $MgCl_2$ were attributable to the Mg^{2+} ion.

In the presence of Mg^{2+}, EGCG decreased the V_{MAX} value of DNMT1-mediated DNA methylation, but it basically did not affect its K_M value, thus suggesting that EGCG predominantly functions as a noncompetitive inhibitor of DNA methylation. One representative data set is shown in **Fig. 9**. Taken into consideration all the data we gathered, it becomes quite clear that the strong inhibitory effect of EGCG on human DNMT1-mediated DNA methylation was independent of the COMT-mediated methylation of EGCG, but it is mainly attributable to its strong, direct inhibition of this enzyme, and the inhibition is greatly enhanced by Mg^{2+}.

Computational analysis of the interaction of EGCG with human DNMT1

To gain insights into the molecular mechanism of DNMT inhibition by EGCG, computational modeling studies were also conducted. A comparison of the X-ray structures of the Class I DNMTs showed that they shared highly similar structures, especially in the catalytic core

Molecular Pharmacology Fast Forward. Published on July 21, 2005 as DOI: 10.1124/mol.104.008367
This article has not been copyedited and formatted. The final version may differ from this version.

regions, which consist of several conserved α-helical and β-sheet structures (Schubert et al., 2003). From analyzing the multiple sequence alignments of several known DNMTs, it became apparent that the human DNMT1 contained unique, long variable regions, which made it more difficult to predict its conformations solely based on computational modeling analysis. Guided by the *Profiles-3D* scores for determining the best conformations for the variable regions, a homology model for human DNMT1 was constructed by using the lowest energy conformations. **Fig. 10A** shows the mode that was developed in the present study for EGCG binding in the catalytic core region of the human DNMT1. In this binding mode, the key binding site residues on human DNMT1 included those that are within the 3-Å reach of the bound EGCG molecule, i.e., Pro1224, Cys1225, Phe1228, Glu1265, Asn1266, Val1267, Arg1309, Arg1310, Arg1311, Val478, Gly1481, Lys1482, and Asn1577. Four of these residues are predicted to form H-bonds with EGCG, which include Glu1265 (O_ε with the *D*-ring OH), Arg1310 (N_{amide} with the *B*-ring OH), Arg1311 (N_ε with the *B*-ring OH, and N_{NH_2} with the *D*-ring OH), and Lys1482 (N_{amide} with the *A*-ring OH).

From the initial binding energy analyses of the EGCG binding conformations using the *CVFF* in the *Affinity* docking program, we predicted that the presence of Mg^{2+} would alter EGCG's binding energy and accordingly, its inhibitory activity. A more detailed calculation of the binding energy was then performed using a model system built in the present study that was composed of EGCG and a group of key catalytic site residues from the DNMT1. The PM3-derived binding energy values (ΔE_{bind}, in kcal/mol) for the formation of complexes between EGCG and DNMT1 in the absence and presence of Mg^{2+} are summarized in **Table 2**. The ΔE_{bind} value for the formation of EGCG-DNMT1 complex in the absence of Mg^{2+} was calculated to be -5.7 kcal/mol, indicating that the binding of EGCG to DNMT1 would be energetically favored even in the absence of Mg^{2+}. This prediction is certainly consistent with our experimental observation that EGCG inhibited DNMTs in the absence of Mg^{2+}. However, in the presence of Mg^{2+}, the ΔE_{bind} value for the formation of DNMT1-EGCG complex was only at -8.1 kcal/mol when three coordinated water molecules were also present (**Table 2** and **Fig. 10B**.). The difference in the binding energy values in the presence

Molecular Pharmacology Fast Forward. Published on July 21, 2005 as DOI: 10.1124/mol.104.008367
This article has not been copyedited and formatted. The final version may differ from this version.

and absence of Mg^{2+} clearly suggests that Mg^{2+} coordination in the catalytic site of DNMT1 would markedly enhance the binding force between EGCG and the enzyme (as many as ~250-fold increase in the computed binding force) by stabilizing their binding interactions. This information is in accord with our experimental observations described in the present study which showed that the presence of Mg^{2+} at 2 mM markedly increased the apparent inhibition potency of EGCG by ~10-fold (refer to **Fig. 8D**).

Molecular Pharmacology Fast Forward. Published on July 21, 2005 as DOI: 10.1124/mol.104.008367
This article has not been copyedited and formatted. The final version may differ from this version.

DISCUSSION

In the present study, we examined several representative catechol-containing dietary polyphenols (tea catechins and bioflavonoids) for their activity in inhibiting DNA methylation catalyzed by *Sss*I DNMT and human DNMT1. Our data showed that all these dietary polyphenols are capable of inhibiting DNMT-mediated DNA methylation *in vitro*, but with varying potencies and efficacies. Notably, among all the dietary polyphenols tested in this study, EGCG was found to be a more potent and efficacious inhibitor of enzymatic DNA methylation *in vitro*. The IC_{50} values for its inhibition of *Sss*I DNMT- and DNMT1-mediated DNA methylation were 0.21 and 0.47 μM, respectively (**Fig. 2**). Additional experiments using cultured MCF-7 and MDA-MB-231 breast cancer cells also showed that treatment with nontoxic concentrations of EGCG or catechin partially inhibited the methylation status of the promoter regions of RARβ gene. Notably, while EGCG was more potent and efficacious than catechin, the differences in their potency and efficacy appeared to be not as pronounced as the results from the *in vitro* DNMT inhibition experiments. As explained below, this may be partially attributable to the fact that catechin is a far better substrate for COMT than EGCG (Zhu et al., 2000; Zhu et al., 2001), which may contribute to an increased intracellular pool of SAH. Also, EGCG usually has a relatively lower intracellular bioavailability than catechin because the former generally has a faster metabolic breakdown.

Our earlier studies have shown that many of the catechol-containing dietary polyphenols are excellent substrates for the *O*-methylation by human or rodent COMT (Zhu et al., 1996; Zhu and Liehr, 1996; Zhu et al., 2000; Zhu et al., 2001). Mechanistically, we hypothesized that these dietary catechols, regardless of whether or not they can also exert a direct inhibition of the DNMTs, may cause an indirect inhibition of the DNMT-mediated DNA methylation through increased formation of SAH (a potent noncompetitive inhibitor of the DNMTs) during their methylation metabolism by COMT. This mechanistic explanation (illustrated in **Fig. 1**) is supported by our data showing that

Molecular Pharmacology Fast Forward. Published on July 21, 2005 as DOI: 10.1124/mol.104.008367
This article has not been copyedited and formatted. The final version may differ from this version.

co-presence of a complete COMT methylation system strongly enhanced the inhibition potency and efficacy of those dietary polyphenols that are suitable substrates for COMT.

Interestingly, the results of our present study also revealed that the strong, direct inhibition of DNA methylation by EGCG is independent of COMT but instead is dependent on the presence of Mg^{2+}. This was particularly the case with respect to human DNMT1. Notably, a recent study reported that the apparent K_I value for inhibition of the human DNMT-mediated DNA methylation by EGCG *in vitro* was ~7 μM, with IC_{50} of ~20 μM (Fang et al., 2003). This value was obtained by using a nuclear fraction (rich in human DNMT1) under reaction conditions where Mg^{2+} was not present. Our data showed that the presence of physiologically-relevant concentrations of Mg^{2+} (such as 2 mM) drastically enhanced the inhibitory potency of EGCG in human DNMT1-mediated DNA methylation reaction *in vitro* by decreasing its IC_{50} value from the previously-reported 20 μM to ~0.5 μM (a ~40-fold increase in potency).

To shed light on the mechanism of DNMT1 inhibition at the molecular level, we also conducted computational modeling analyses to probe the interactions between EGCG and human DNMT1. Consistent with the recently proposed binding site model of human DNMT1 for EGCG (Fang et al., 2003), we identified Glu1265 as one of the key catalytic site residues that interact with EGCG by forming H-bonds. However, our binding mode predicted that the *p*-OH group of EGCG's *D*-ring (the gallic acid moiety) would form an H-bond with Glu1265, while the model by Fang et al. (2003) suggested that the same amino acid residue would form an H-bond with one of the *m*-OH groups of the *D*-ring. We believe that the *p*-OH oxygen on the *D*-ring would be a better donor for the formation of H-bonding with Glu1265 than the corresponding *m*-OH oxygen due to its stronger acidity.

In addition, the data from our modeling studies suggest that Mg^{2+} likely is coordinated to Glu1265 at the catalytic core site. This conclusion was, in part, derived from a detailed comparison of the active-site conformations of the human DNMT1 with the COMT protein using multiple

Molecular Pharmacology Fast Forward. Published on July 21, 2005 as DOI: 10.1124/mol.104.008367
This article has not been copyedited and formatted. The final version may differ from this version.

modeling tools, and we suggested that Glu1265 on human DNMT1 likely is equivalent to one of the two conserved acidic residues in COMT that are known to coordinate Mg^{2+} (Vidgren et al., 1994). Based on our proposed mode of interactions between EGCG and DNMT1 (**Fig. 10**), detailed binding energy calculations revealed that the formation of the EGCG-DNMT1 complex in the presence of Mg^{2+} would be much preferred over the complex without Mg^{2+} ($\Delta\Delta E_{bind}$ = -2.4 kcal/mol, **Table 2**), and it was estimated that EGCG's inhibitory potency would be markedly enhanced in the presence of Mg^{2+} compared to that in the absence of Mg^{2+}. This estimate, albeit indirectly derived from computations based on our predicted mode of interactions, is perfectly in agreement with our experimental observation described in the present study.

Here it is of interest to point out that myricetin, which has a pyrogallic acid moiety (similar to the gallic acid moiety of EGCG), also showed a stronger inhibition potency and efficacy than quercetin and fisetin in the presence of Mg^{2+}. These experimental data are in agreement with the conclusion based on our modeling studies that the gallic acid moiety of EGCG plays a crucial role in its high-affinity interaction with the catalytic site of human DNMT1. In comparison, in the cases of catechin, epicatechin, quercetin, and fisetin which all lack a gallic/pyrogallic acid moiety, they cannot form a similarly strong coordination with Mg^{2+} and Glu1265. Therefore, these four catechol-containing dietary polyphenols would have a weaker direct inhibition of the DNMTs as predicted according to our modeling data, but they could still exert a considerably strong indirect inhibition of the DNMTs through the formation of SAH during their metabolic methylation by COMT.

It is known that hypermethylation of DNA is a key epigenetic mechanism for the silencing of many genes including those of tumor suppressors, DNA repair enzymes, and receptors (Esteller, 2002; Jones and Baylin, 2002; Jones and Takai, 2001; Lichtenstein and Kisseljova, 2001). Several tumor suppressor and receptor genes have been reported to be hypermethylated and transcriptionally silenced during the development of different types of cancers. It has been suggested that inhibition of DNMTs, along with inhibition of the histone deacetylase, may prevent the hypermethylation and silencing of these key genes, and this inhibition may contribute to the treatment of cancer and/or

Molecular Pharmacology Fast Forward. Published on July 21, 2005 as DOI: 10.1124/mol.104.008367
This article has not been copyedited and formatted. The final version may differ from this version.

prevention of carcinogenesis. Considerable initial research efforts have already been made in this direction in recent years (Zhou et al., 2002; Bovenzi and Momparlar, 2001; Asparcio et al., 2003; Shi et al., 2003; Saunders et al., 1999; Shaker et al., 2003; Yoshida et al., 2001). For instance, there are data showing a reduced intestinal tumorigenesis due to DNMT1 deficiency and use of 5-aza-2'-deoxycytidine in the *MIN* mice, which carry a mutated *APC* gene (Laird et al., 1995; Eads et al., 2002).

Animals studies have shown that oral administration of green tea could inhibit chemical carcinogenesis in some organs, and it is believed that multiple mechanisms are involved (Lu et al., 2001). However, it remains to be determined whether and to what extent this cancer-preventive activity is due to the inhibition of DNMTs by EGCG. Based on a recent report of the very high K_I and IC_{50} values (6.89 μM and 20 μM, respectively) of EGCG, it was accordingly suggested that these effective concentrations are much higher than those achievable in the internal organs, but might only be achievable in the oral cavity (in the saliva), stomach, esophagus, and intestines where there is direct contacts between EGCG and the epithelial cells. However, in light of the new results from our present study showing lower IC_{50} values (at submicromolar concentrations) of EGCG for inhibition of human DNMT1-mediated DNA methylation *in vitro* and in cultured cancer cells, our finding may increase the possibility that tea polyphenols may be able to regulate DNA methylation status even in the internal organs.

Lastly, it is of considerable interest to point out that a strong inhibition of DNA methylation by catechol-containing dietary polyphenols may also represent an antibacterial mechanism, especially in those bacteria that express high levels of COMT-like enzymes for the rapid methylation of dietary catechols and also for the formation of SAH. In Chinese traditional medicine, it is generally believed that drinking tea would generally enhance oral hygiene. Modern experimental studies have also suggested that drinking tea would inhibit bacterial growth in the oral cavity. However, it remains to be determined whether this inhibition of bacterial growth is partly due to a strong inhibition of their DNA methylation.

Molecular Pharmacology Fast Forward. Published on July 21, 2005 as DOI: 10.1124/mol.104.008367
This article has not been copyedited and formatted. The final version may differ from this version.

In summary, tea catechins (catechin, epicatechin, and EGCG) and bioflavonoids (quercetin, fisetin, and myricetin) each inhibited *Sss*I DNMT- and DNMT1-mediated DNA methylation. The IC_{50} values for the *in vitro* inhibition of human DNMT1 by catechin, epicatechin and various flavonoids ranged from 1.0 – 8.4 μM, but EGCG was a more potent inhibitor, with IC_{50} values at 0.21 – 0.47 μM. Kinetic analyses suggested that catechol-containing dietary polyphenol could inhibit DNA methylation through two mechanisms: direct inhibition of the DNMTs plus indrect inhibition of the enzymes through increased formation of SAH (a potent noncompetitive inhibitor of DNMTs) during COMT-mediated *O*-methylation of the catecholic dietary polyphenols. However, the strong inhibitory activity of EGCG for human DNMT1-mediated DNA methylation was largely independent of its own methylation, and it is essentially due to a Mg^{2+}-dependent direct inhibition of the enzyme.

Molecular Pharmacology Fast Forward. Published on July 21, 2005 as DOI: 10.1124/mol.104.008367
This article has not been copyedited and formatted. The final version may differ from this version.

REFERENCES

Aparicio A, Eads CA, Leong LA, Laird PW, Newman EM, Synold TW, Baker SD, Zhao M, and Weber JS (2003) Phase I trial of continuous infusion 5-aza-2'-deoxycytidine. *Cancer Chemother Pharmacol* **51:**231-239.

Bestor TH, and Ingram VM (1983) Two DNA methyltransferases from murine erythroleukemia cells: purification, sequence specificity, and mode of interaction with DNA. *Proc Natl Acad Sci U S A* **80:**5559-5563.

Bovenzi V, and Momparler RL (2001) Antineoplastic action of 5-aza-2'-deoxycytidine and histone deacetylase inhibitor and their effect on the expression of retinoic acid receptor β and estrogen receptor α genes in breast carcinoma cells. *Cancer Chemother Pharmacol* **48**:71-76.

Bowie JU, Lüthy R, and Eisenberg D (1991) A method to identify protein sequences that fold into a known three-dimensional structure. *Science* **253:**164-170.

Chen RZ, Pettersson U, Beard C, Jackson-Grusby L, and Jaenisch R (1998). DNA hypomethylation leads to elevated mutation rates. *Nature,* **395:**89-93.

Dauber-Osguthorpe P, Roberts VA, Osguthorpe DJ, Wolff J, Genest M, and Hagler AT (1998) Structure and energetics of ligand binding to proteins: Escherichia coli dihydrofolate reductase-trimethoprim, a drug-receptor system. *Proteins* **4:**31-47.

Ding HQ, Karasawa N, and Goddard WAIII (1992) Atomic level simulations on a million particles: The cell multipole method for Coulomb and London nonbond interactions. *J Chem Phys* **97:**4309-4315.

Dudev T, and Lim C (2003) Principles governing Mg, Ca, and Zn binding and selectivity in proteins. *Chem Rev* **103:**773-787.

Eads CA, Nickel AE, and Laird PW (2002) Complete genetic suppression of polyp formation and reduction of CpG-island hypermethylation in Apc(Min/+) Dnmt1-hypomorphic mice. *Cancer Res* **62:**1296-1299.

Esteller M (2002) CpG island hypermethylation and tumor suppressor genes: a booming present, a brighter future. *Oncogene* **21:**427-5440.

Fang MZ, Wang Y, Ai N, Hou Z, Sun Y, Lu H, Welsh W, and Yang CS (2003) Tea polyphenol (-)-epigallocatechin-3-gallate inhibits DNA methyltransferase and reactivates methylation-silenced gene in cancer cell lines. *Cancer Res* **63:**7563-7570.

Fiser A, Do RK, and Sali A (2000) Modeling of loops in protein structures. *Protein Sci* **9**:1753-1773.

Higgins DG, Thompson JD, and Gibson TJ (1996) Using CLUSTAL for multiple sequence alignments. *Methods Enzymol* **266:**383-402.

James SJ, Melnyk S, Pogribna M, Pogribny IP, and Caudill MA (2002) Elevation in *S*-adenosylhomocysteine and DNA hypomethylation: potential epigenetic mechanism for homocysteine-related pathology. *J Nutr* **132:**2361s-2366s.

Jones PA, and Baylin SB (2002) The fundamental role of epigenetic events in cancer. *Nat Rev Genet* **3:**415-428.

Jones PA, and Takai D (2001) The role of DNA methylation in mammalian epigenetics. *Science (Wash. DC)* **293:**1068-1070.

Laird PW, Jackson-Grusby L, Fazeli A, Dickinson SL, Jung WE, Li E, Weinberg RA, and Jaenisch R (1995) Suppression of intestinal neoplasia by DNA hypomethylation. *Cell* **81:**197-205.

Lichtenstein AV, and Kisseljova NP (2001) DNA methylation and carcinogenesis. *Biochemistry (Mosc.)* **66:**235-255.

Liu ZJ, and Zhu BT (2004) Concentration-dependent mitogenic and antiproliferative actions of 2-methoxyestradiol in estrogen receptor-positive human breast cancer cells. *J Steroid Biochem Mol Biol* **88:**265-275.

Lu YP, Lou YR, Lin Y, Shih WJ, Huang MT, Yang CS, and Conney AH (2001) Inhibitory effects of orally administered green tea, black tea, and caffeine on skin carcinogenesis in mice previously treated with ultraviolet B light (high-risk mice): relationship to decreased tissue fat. *Cancer Res* **61:**5002-5009.

Martin JL, and McMillan FM (2002) SAM (dependent) I AM: The *S*-adenosylmethionine-dependent methyltransferase fold. *Curr Opin Struct Biol* **12:**783-793.

Okano M, Xie S, and Li E (1998) Cloning and characterization of a family of novel mammalian DNA (cytosine-5) methyltransferases. *Nat Genet* **19**:219-220.

Palmisano WA, Divine KK, Saccomanno G, Gilliland FD, Baylin SB, Herman JG, and Belinsky SA (2000) Predicting lung cancer by detecting aberrant promoter methylation in sputum. *Cancer Res* **60:**5954-5958.

Press WH, Teukolsky SA, Vetterling WT, and Flanery BP (1993) Numerical Recipes – The art of scientific computing pp 420-424, Cambridge Univ Press, Cambridge.

Renbaum P, Abrahamove D, Fainsod A, Wilson GG, Rottem S, and Razin A (1990) Cloning, characterization, and expression in Escherichia coli of the gene coding for the CpG DNA methylase from Spiroplasma sp. strain MQ1(M.SssI). *Nucleic Acids Res* **18:**1145-1152.

Saunders N, Dicker A, Popa C, Jones S, and Dahler A (1999) Histone deacetylase inhibitors as potential anti-skin cancer agents. *Cancer Res* **59:**399-404.

Schubert HL, Blumenthal RM, and Cheng X (2003) Many paths to methyltransfer: a chronicle of convergence. *Trends Biochem Sci* **28**:329-335.

Shaker S, Bernstein M, Momparler LF, and Momparler RL (2003) Preclinical evaluation of antineoplastic activity of inhibitors of DNA methylation (5-aza-2'-deoxycytidine) and histone deacetylation (trichostatin A, depsipetide) in combination against myeloid leukemic cells. *Leuk Res* **27:**437-444.

Shi H, Wei SH, Leu YW, Rahmatpanah F, Liu JC, Yan PS, Nephew KP, and Huang TH (2003) Triple analysis of the cancer epigenome: an integrated microarray system for assessing gene expression, DNA methylation, and histone acetylation. *Cancer Res* **63**:2164-2171.

Sirchia SM, Ferguson AT, Sironi E, Subramanyan S, Orlandi R, Sukumar S, and Sacchi N (2000) Evidence of epigenetic changes affecting the chromatin state of the retinoic acid receptor beta2 promoter in breast cancer cells. *Oncogene* **19:**1556-1563.

Stewart JJJ (1989) Optimization of parameters for semiempirical methods. I. Method. *J Comp Chem* **10:**209-220.

Vidgren J, Svensson LA, and Liljas A (1994) Crystal structure of catechol *O*-methyltransferase. *Nature* **368:**354-358.

Wainfan E, and Poirier LA (1992) Methyl groups in carcinogenesis: effects on DNA methylation and gene expression. *Cancer Res* **52:**2071s-2077s.

Yoshida M, Furumai R, Nishiyama M, Komatsu Y, Nishino N, and Horinouchi S (2001) Histone deacetylase as a new target for cancer chemotherapy. *Cancer Chemother Pharmacol* **48(Suppl. 1):**S20-S26.

Zhou L, Cheng X, Connolly BA, Dickman MJ, Hurd PJ, and Hornby DP (2002) Zebularine: a novel DNA methylation inhibitor that forms a covalent complex with DNA methyltransferases. *J Mol Biol* **321:**591-599.

Zhu BT, Ezell EL, and Liehr JG (1996) Catechol-*O*-methyltransferase-catalyzed rapid *O*-methylation of mutagenic flavonoids. Metabolic inactivation as a possible reason for their lack of carcinogenicity *in vivo*. *J Biol Chem* **269:**292-299.

Zhu BT, and Liehr JG (1996) Inhibition of catechol *O*-methyltransferase-catalyzed *O*-methylation of 2- and 4-hydroxyestradiol by quercetin. Possible role in estradiol-induced tumorigenesis. *J Biol Chem* **271:**1357-1363.

Zhu BT, Patel UK, Cai MX, and Conney AH (2000) *O*-Methylation of tea polyphenols catalyzed by human placental cytosolic catechol-*O*-methyltransferase. *Drug Metab Dispos* **28:**1024-1030.

Zhu BT, Patel UK, Cai MX, Lee AJ, and Conney AH (2001) Rapid conversion of tea catechins to monomethylated products by rat liver cytosolic catechol-*O*-methyltransferase. *Xenobiotica* **31:**879-890.

FOOTNOTES:

1. Frank and Josie P. Fletcher Professor of Pharmacology and an American Cancer Society Research Scholar, and to whom requests for reprints should be addressed at the Department of Basic Pharmaceutical Sciences, College of Pharmacy, University of South Carolina, Room 617 of Coker Life Sciences Building, 700 Sumter Street, Columbia, SC 29208 (USA).

PHONE: 803-777-4802; FAX: 803-777-8356; E-MAIL: BTZhu@cop.sc.edu

2. Abbreviations used: DNMT, DNA methyltransferase; COMT, catechol-*O*-methyltransferase; SAM, *S*-adenosyl-*L*-methionine; SAH, *S*-adenosyl-*L*-homocysteine; EGCG, (-)-epigallocatechin-3-*O*-gallate.

Molecular Pharmacology Fast Forward. Published on July 21, 2005 as DOI: 10.1124/mol.104.008367
This article has not been copyedited and formatted. The final version may differ from this version.

FIGURE LEGENDS

Figure 1 The DNMT-mediated DNA methylation and its modulation by dietary catechols. As shown in *panel A*, both DNMT-mediated DNA methylation and COMT-mediated O-methylation of dietary catechols use SAM as the methyl donor. During the methylation of various catechol-containing dietary polyphenols, the formation of SAH would be markedly increased. Since SAH is an effective feedback inhibitor of various SAM-dependent methylation reactions, it is hypothesized that the elevated intracellular levels of SAH as a result of the metabolic O-methylation of various dietary catechols may cumulatively cause a significant inhibition of the DNMT-mediated DNA methylation. The chemical structures of several dietary catechol-containing polyphenols used in this study are shown in *panel B*.

Figure 2 Inhibition of *Sss*I DNMT- and DNMT1-mediated DNA methylation by different concentrations of catechin, epicatechin, and EGCG. The incubation conditions are described under "**Materials and Methods**." The concentrations of COMT used in the *Sss*I DNMT- and DNMT1-mediated DNA methylation reactions were 2 and 4 units/25 μl, respectively, and the final concentrations of $MgCl_2$ were 10 mM and 2 mM, respectively. The concentrations of three tea catechins used in this experiment ranged from 0.1 to 20 μM. *Filled circles*, the reaction without COMT. *Open circles*, the reaction with COMT. Reactions were carried out at 37°C for 30 min. Most data points represent the mean ± SE of 3-5 determinations.

Figure 3 Inhibition of *Sss*I DNMT- and DNMT1-mediated DNA methylation by varying concentrations of quercetin, fisetin, and myricetin. The incubation conditions are described under "**Materials and Methods**." The concentrations of COMT used in the *Sss*I DNMT- and DNMT1-mediated DNA methylation reactions were 2 and 4 units/25 μl, respectively, and the final concentrations of $MgCl_2$ were 10 mM and 2 mM, respectively. The concentrations of three bioflavonoids ranged from 0.5 to 20 μM. *Filled circles*, the reaction without COMT. *Open circles*, the reaction with COMT. Reactions were carried out at 37°C for 30 min. Most data points represent the mean ± SE of 3-5 determinations.

Figure 4 The morphology of MCF-7 and MDA-MB-231 cells treated with EGCG or catechin. The concentrations of EGCG or catechin used were as indicated, and the length of the treatment was 6 days for MCF-7 cells, and 3 days for MDA-MB-231 cells.

Figure 5 Methylation status of the promoter regions of the RARβ gene in MCF-7 and MDA-MB-231 cells treated with catechin or EGCG. The MDA-MB-231 and MCF-7 cells were treated with 0, 0.2, 1, 5, 25, or 50 μM of catechin or EGCG for 3 and 6 days, respectively. For each cell line, the upper bar graphs represent changes in the unmethylation-specific bands, and the lower bar graphs represent changes in the methylation-specific bands. Data are expressed as % of control (i.e.,

Molecular Pharmacology Fast Forward. Published on July 21, 2005 as DOI: 10.1124/mol.104.008367
This article has not been copyedited and formatted. The final version may differ from this version.

normalized to the corresponding control group), and each graph bar represents the mean ± S.E. of 4 parallel replicate experiments. For convenience and simplicity, only one representative set of the unmethylation specific bands (U) and methylation-specific bands (M) that were taken from 4 parallel replicate experiments were shown.

Figure 6 Eadie-Hofstee plots for the inhibitory effect of epicatechin on DNA methylation by *Sss*I DNMT (*Panel A*) and human DNMT1 (*Panel B*). The methylation of DNA in the presence of epicatechin was dependent on the substrate concentration (*left insets*). The incubation conditions are described under "**Materials and Methods**." COMT (2 units/25 µl for *Sss*I DNMT and 4 units/25 µl for human DNMT1) and $MgCl_2$ (10 mM for *Sss*I DNMT and 2 mM for human DNMT1) were added. The reactions were carried out at 37°C for 30 min. Each data point was the means of duplicate measurements.

Figure 7 The effect of SAH on human DNMT1-mediated DNA methylation. *Upper panel:* Inhibition of human DNMT1-mediated DNA methylation by SAH. The incubation mixture consisted of 1 µM poly(dI-dC)·poly(dI-dC), 5 µM [methyl-^{3}H]SAM, 0-5 µM SAH, and 1 unit/25 µl of DNMT1 in a final volume of 25 µl. *Lower panel:* The *left panel* illustrates the rate of DNMT1-mediated DNA methylation as a function of poly(dI-dC)·poly(dI-dC) concentrations in the presence or absence of SAH. The *right panel* shows the Eadie-Hofstee plot of the same data set. The reaction conditions consisted of 0.04-1.25 µM poly(dI-dC)·poly(dI-dC), 5 µM [methyl-^{3}H]SAM, SAH (at 0, 0.2, and 0.625 µM), and 1 unit/25 µl of human DNMT1 in a final volume of 25 µl. Incubations were carried out at 37°C for 30 min in the presence of 2 mM $MgCl_2$. Each data point was derived from at least two replicate measurements.

Figure 8 Inhibition of *Sss*I DNMT- and human DNMT1-mediated DNA methylation by different concentrations of $MgCl_2$ and EGCG. *Upper Panel:* Direct inhibition of *Sss*I DNMT-mediated DNA methylation by $MgCl_2$ (at 0.5, 1.0, 2.0, 4.0, and 10 mM) in the absence of COMT (*A*), and the direct inhibition by EGCG in the absence or presence of 2 mM $MgCl_2$ (*B*). EGCG concentrations used for inhibiting *Sss*I DNMT activity were 0.1, 1.0, 10, and 20 µM. *Lower Panel:* Direct inhibition of DNMT1-mediated DNA methylation by $MgCl_2$ (at 0.5, 2.0, and 10 mM) in the absence of COMT (*C*), and the direct inhibition by EGCG in the absence or presence of 2 mM $MgCl_2$ (*D*). EGCG concentrations used for inhibiting DNMT1-mediated DNA methylation were 0.05, 0.1, 1.0, and 10 µM. The incubation mixture consisted of 1 µM poly IC, 5 µM [methyl-^{3}H]SAM, and 1 unit/25 µl of DNMT1. Reactions were carried out at 37°C for 30 min. Most data points represent the mean ± SE of 3-5 determinations.

Figure 9 Eadie-Hofstee plots for the inhibition of human DNMT1-mediated DNA methylation by EGCG. The substrate concentration dependence for the *in vitro* DNA methylation in the presence or absence of EGCG is shown in the *left inset*. The incubation conditions are described under

Molecular Pharmacology Fast Forward. Published on July 21, 2005 as DOI: 10.1124/mol.104.008367
This article has not been copyedited and formatted. The final version may differ from this version.

"**Materials and Methods**." The concentration of $MgCl_2$ used was 2 mM. The reactions were carried out at 37°C for 30 min. Each data point was the mean of duplicate determinations.

Figure 10 The EGCG binding interaction with the human DNMT1. *Panel A.* EGCG and DNMT1 binding in the absence of Mg^{2+}. The human DNMT1 is represented in cartoon depiction. Hydrogen bonding interactions between EGCG (in ball-and-stick depiction) and the human DNMT1 residues Glu1265, Arg1310, Arg1311, and Lys1482 (in stick depiction) are represented in green dots. SAM (in stick depiction) is represented with the van der Waals surface (in white dots). α-Helices are colored in cyan, and β-sheets are colored in purple. *Panel B.* EGCG and DNMT1 binding in the presence of Mg^{2+} (in ball depiction) with three coordinated water molecules (in ball depiction). Note that for water molecules, only the oxygen atoms are represented. The distances labeled for the H-bonding in *Panel A* and also for the Mg^{2+}-oxygen coordination in *Panel B* are in the unit of Å. Color coding of EGCG, SAM, and the enzyme catalytic site residues: green, C; red, O; blue, N; yellow, S; magenta, Mg; and white, H.

Molecular Pharmacology Fast Forward. Published on July 21, 2005 as DOI: 10.1124/mol.104.008367
This article has not been copyedited and formatted. The final version may differ from this version.

Table 1. List of primer sequences, annealing temperatures, and expected product sizes for MSP

Gene		Forward Primers (5'-3')	Reverse Primers (5'-3')	Anealing Temp. (°C)	Product Size (bp)
RARβ	N:	TTAAGTTTTGTGAGAATTTTG	CCTATAATTAATCCAAATAATCATTTA CC	53	425
	IC:	AGATTAGTTGGGTTATTTGAA	CATCCCAATCCTCAAACAA	53	198
	U:	TTGAGAATGTGAGTGATTTGA	AACCAATCCAACCAAAACAA	62	146
	M:	TCGAGAACGCGAGCGATTCG	GACCAATCCAACCGAAACGA	62	146

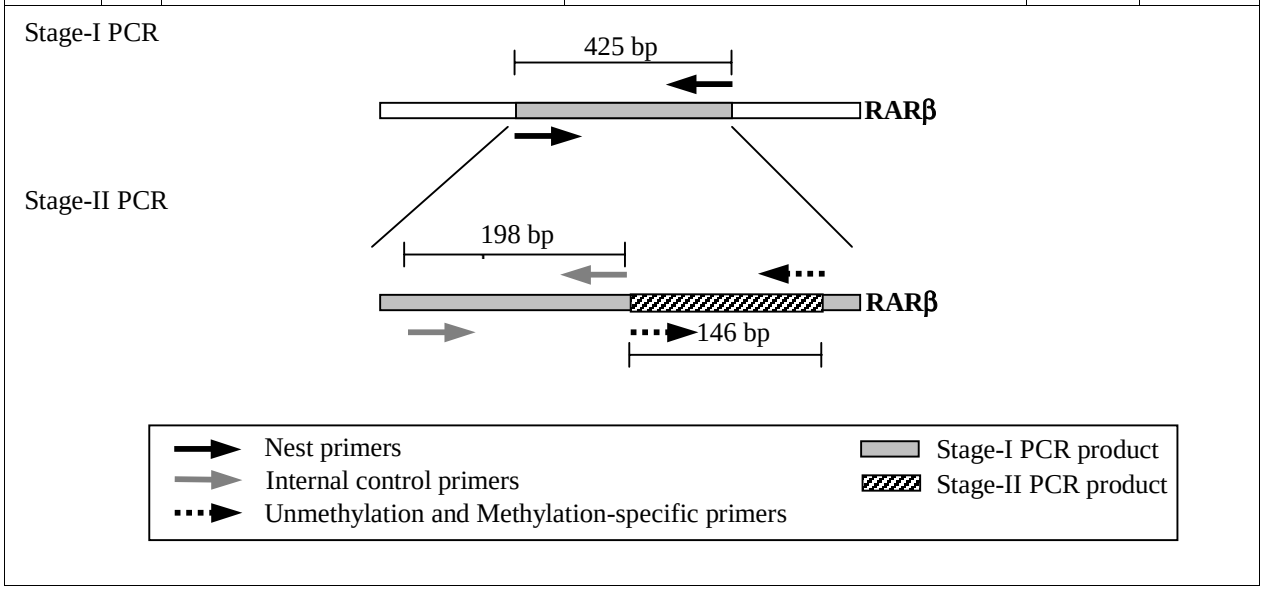

N, nest primers; IC, internal control primers; U, unmethylation-specific primers; and M, methylation-specific primers

Molecular Pharmacology Fast Forward. Published on July 21, 2005 as DOI: 10.1124/mol.104.008367
This article has not been copyedited and formatted. The final version may differ from this version.

Table 2. Comparison of PM3-derived binding energy values (in kcal/mol) for complex formation between the human DNMT1 and EGCG in the absence or presence of Mg^{2+}. As describe in the main text, a model system of the catalytic core region of the human DNMT1 was used. Note that when Mg^{2+} is present, three water molecules were also included in the proposed computational model to satisfy the preferred octahedral coordination geometry of the Mg^{2+} ion.

				Complex	Binding energy[a]	
In the absence of Mg^{2+}					ΔE_{bind}	$\Delta\Delta E_{bind}$
DNMT1	EGCG			DNMT1-EGCG		
-588.0	**-385.0**			**-978.7**	**-5.7**	**0.0**
In the presence of Mg^{2+} and with the coordinated water molecules						
DNMT1	EGCG	Mg^{2+}	3 H_2O	DNMT1- $Mg^{2+}(3H_2O)$-EGCG		
-588.0	**-385.0**	**217.9**	3 x (**-53.4**)	**-923.4**	**-8.1**	**-2.4**

[a]The binding free energy (ΔG_{bind}) was approximated by the ligand-receptor interaction energy (ΔE_{bind}). ΔE_{bind} of MTase-EGCG, for example, was calculated by: $\Delta E_{bind} = E_{complex} - (E_{MTase} + E_{EGCG})$. The relative binding energy ($\Delta\Delta E_{bind}$) for the DNMT1-Mg^{2+}-EGCG complex or the DNMT1-$Mg^{2+}(3H_2O)$-EGCG complex was obtained by using ΔE_{bind} of DNMT1-EGCG, -5.7 kcal/mol, as the reference value.

Molecular Pharmacology Fast Forward. Published on July 21, 2005 as DOI: 10.1124/mol.104.008367
This article has not been copyedited and formatted. The final version may differ from this version.

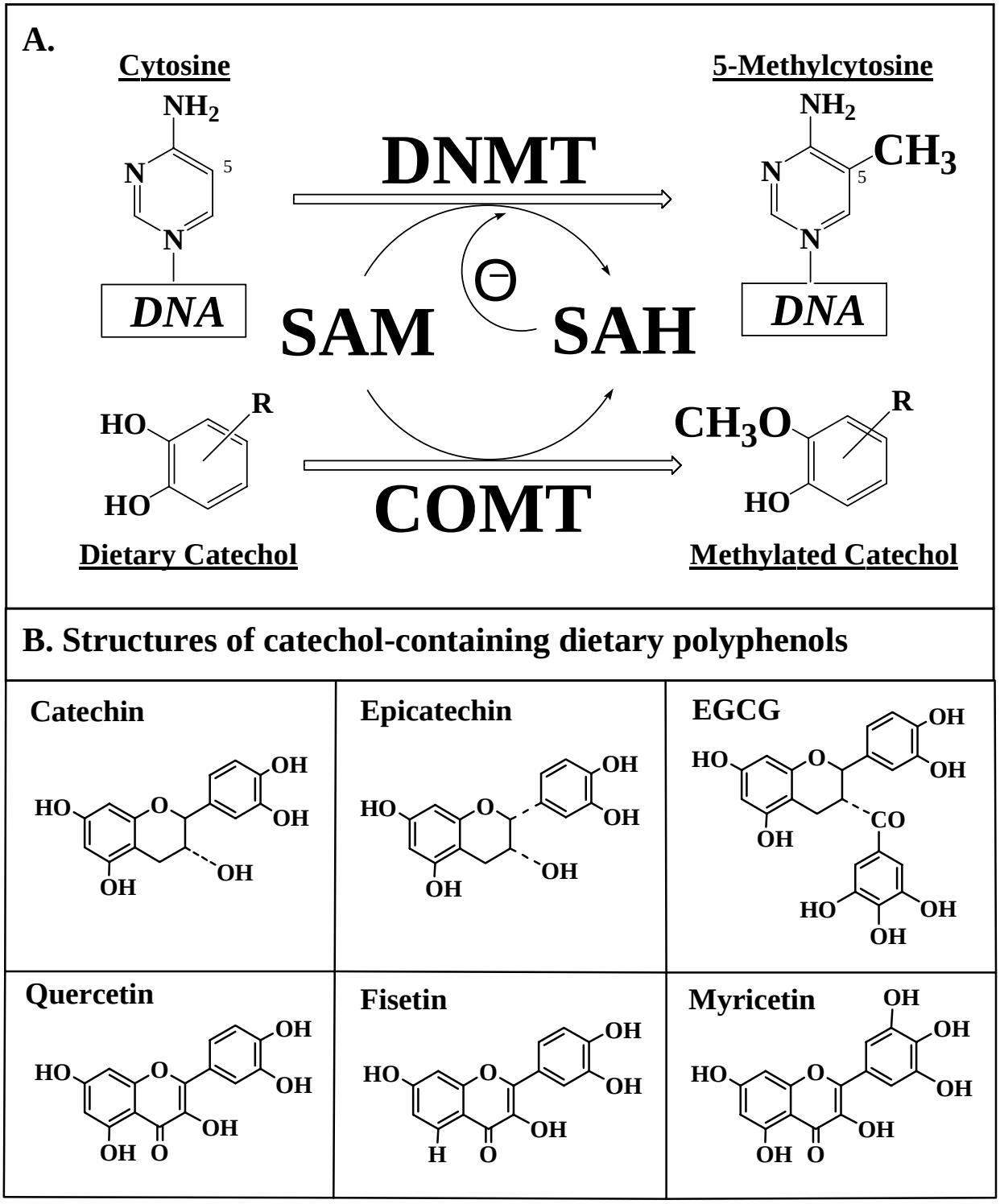

Fig. 1

Molecular Pharmacology Fast Forward. Published on July 21, 2005 as DOI: 10.1124/mol.104.008367
This article has not been copyedited and formatted. The final version may differ from this version.

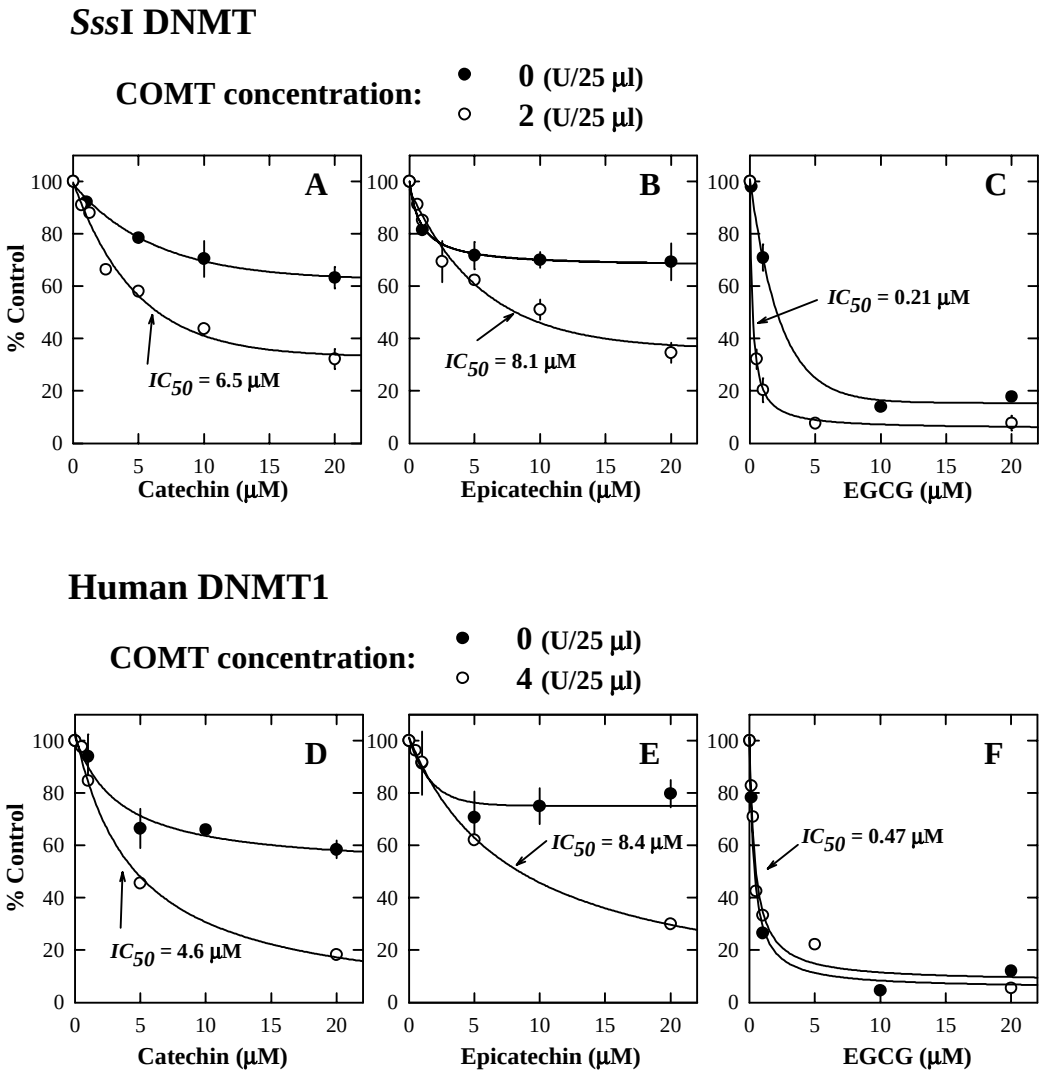

Fig. 2

Molecular Pharmacology Fast Forward. Published on July 21, 2005 as DOI: 10.1124/mol.104.008367
This article has not been copyedited and formatted. The final version may differ from this version.

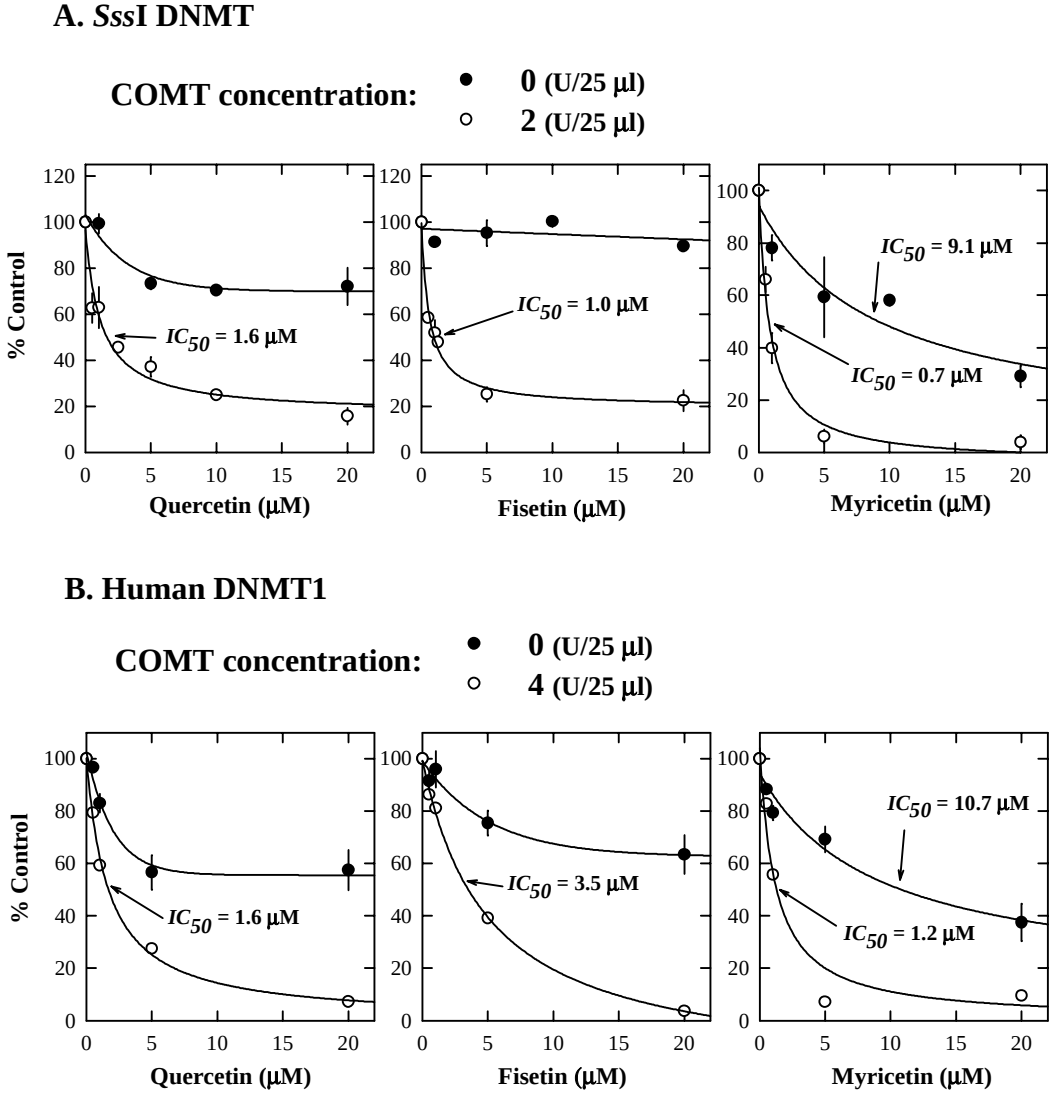

Fig. 3

Molecular Pharmacology Fast Forward. Published on July 21, 2005 as DOI: 10.1124/mol.104.008367
This article has not been copyedited and formatted. The final version may differ from this version.

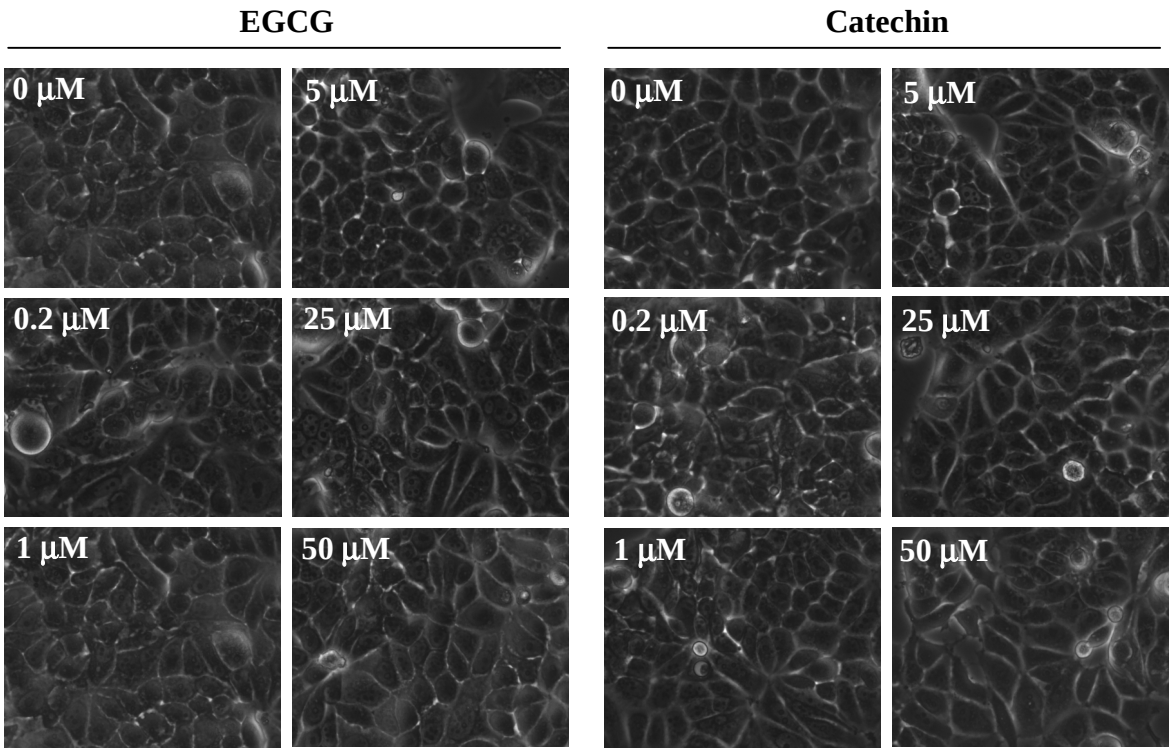

Fig. 4

Molecular Pharmacology Fast Forward. Published on July 21, 2005 as DOI: 10.1124/mol.104.008367
This article has not been copyedited and formatted. The final version may differ from this version.

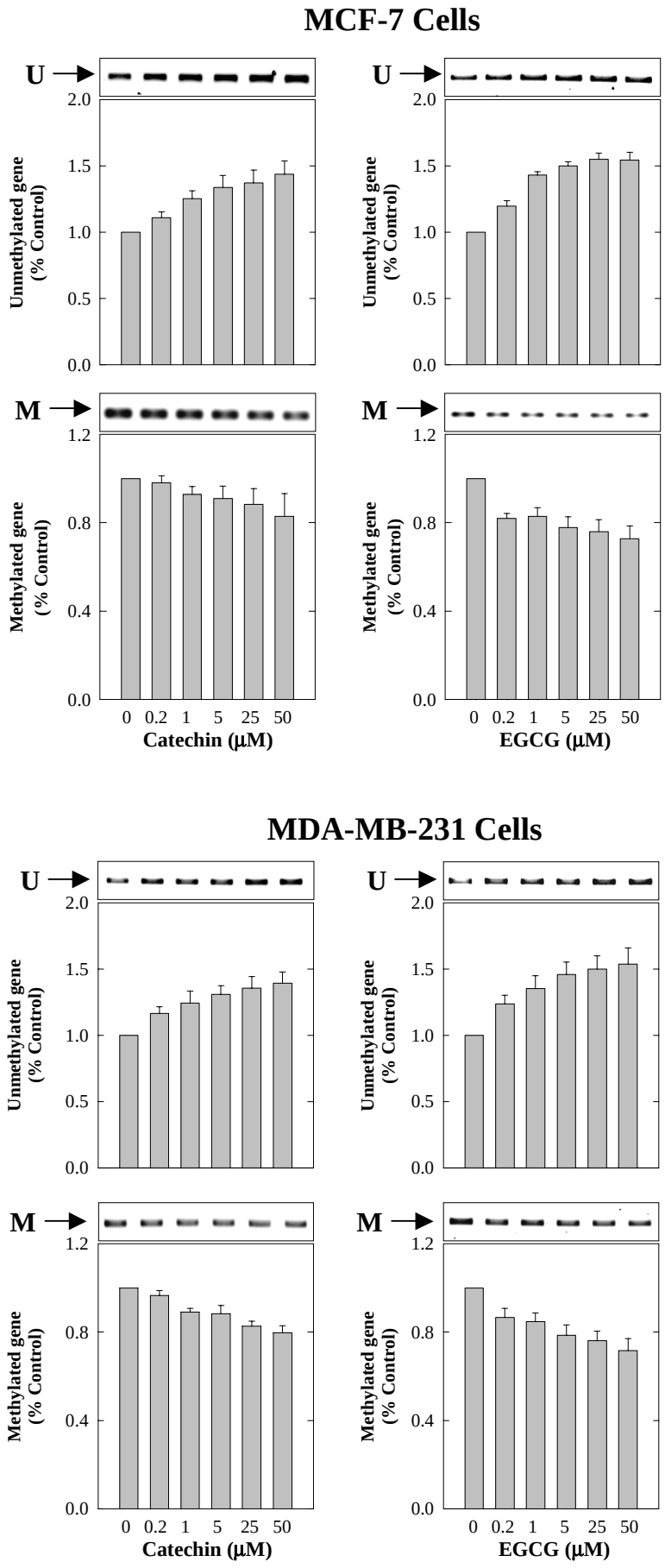

Fig. 5

Molecular Pharmacology Fast Forward. Published on July 21, 2005 as DOI: 10.1124/mol.104.008367
This article has not been copyedited and formatted. The final version may differ from this version.

A. *Sss*I DNMT

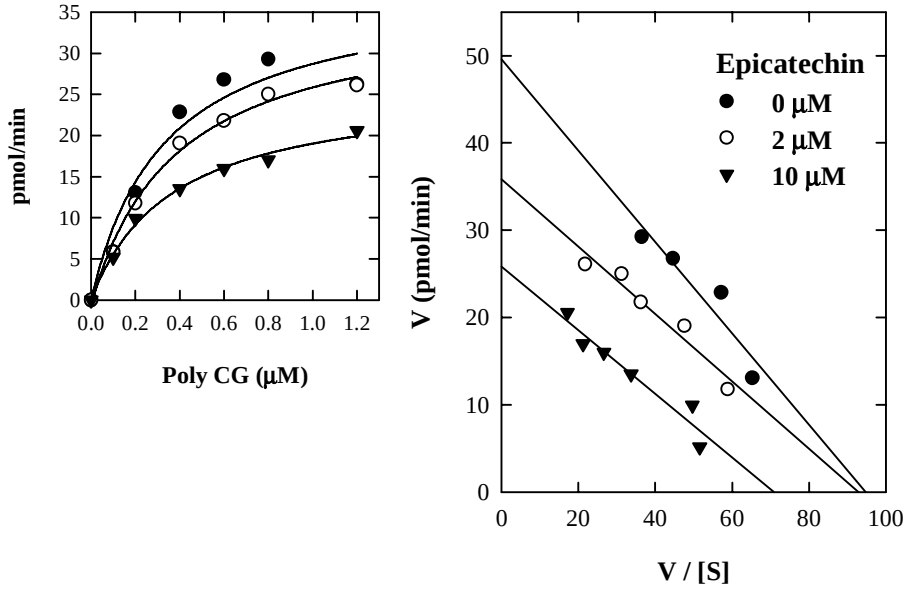

B. Human DNMT1

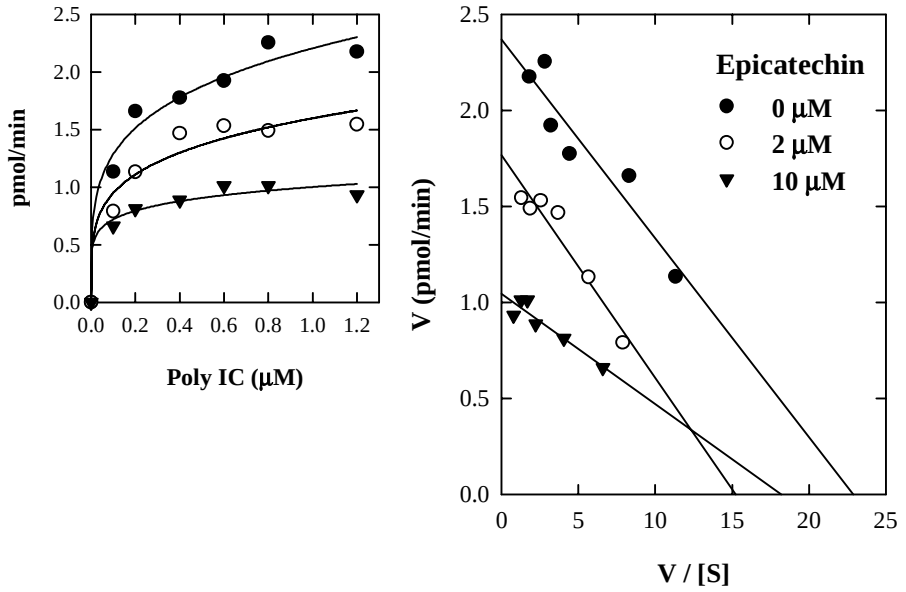

Fig. 6

Molecular Pharmacology Fast Forward. Published on July 21, 2005 as DOI: 10.1124/mol.104.008367
This article has not been copyedited and formatted. The final version may differ from this version.

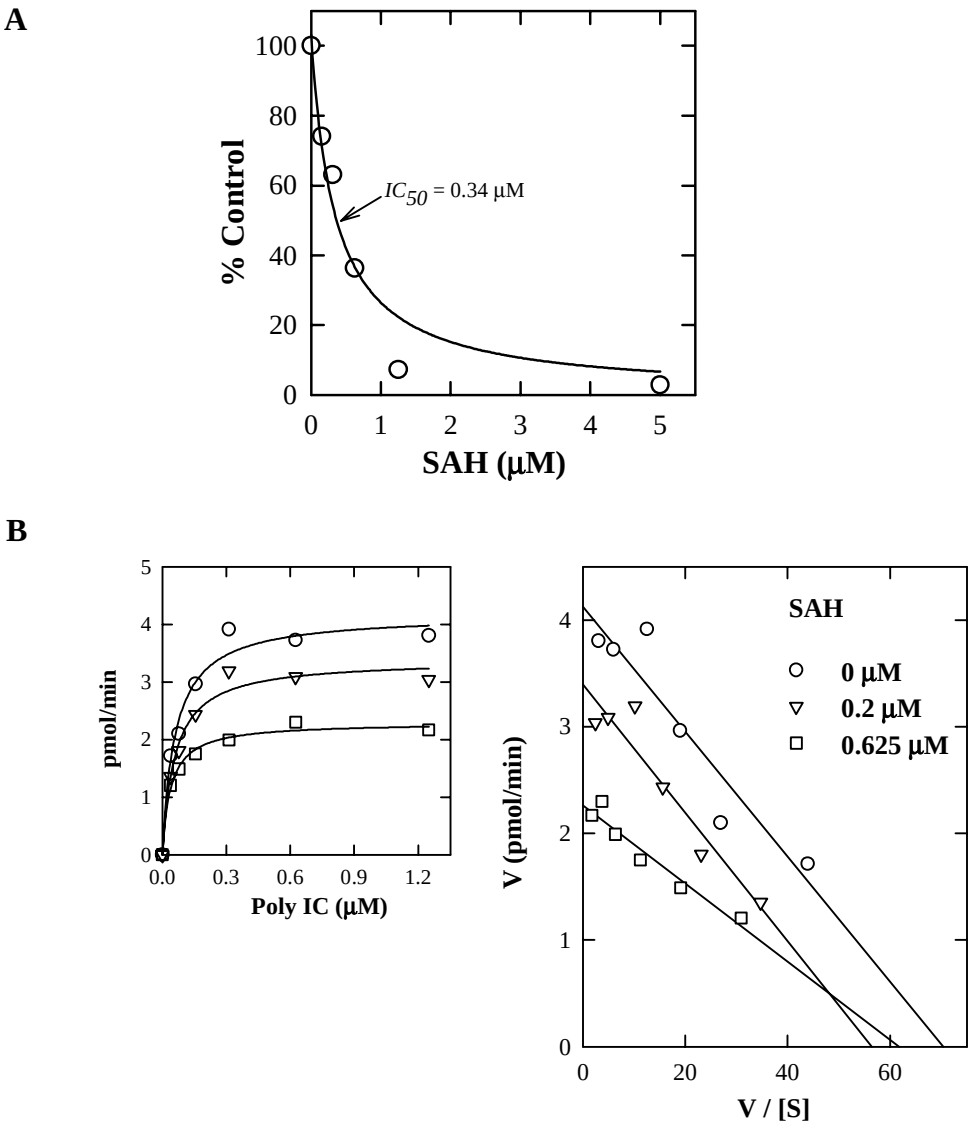

Fig. 7

Molecular Pharmacology Fast Forward. Published on July 21, 2005 as DOI: 10.1124/mol.104.008367
This article has not been copyedited and formatted. The final version may differ from this version.

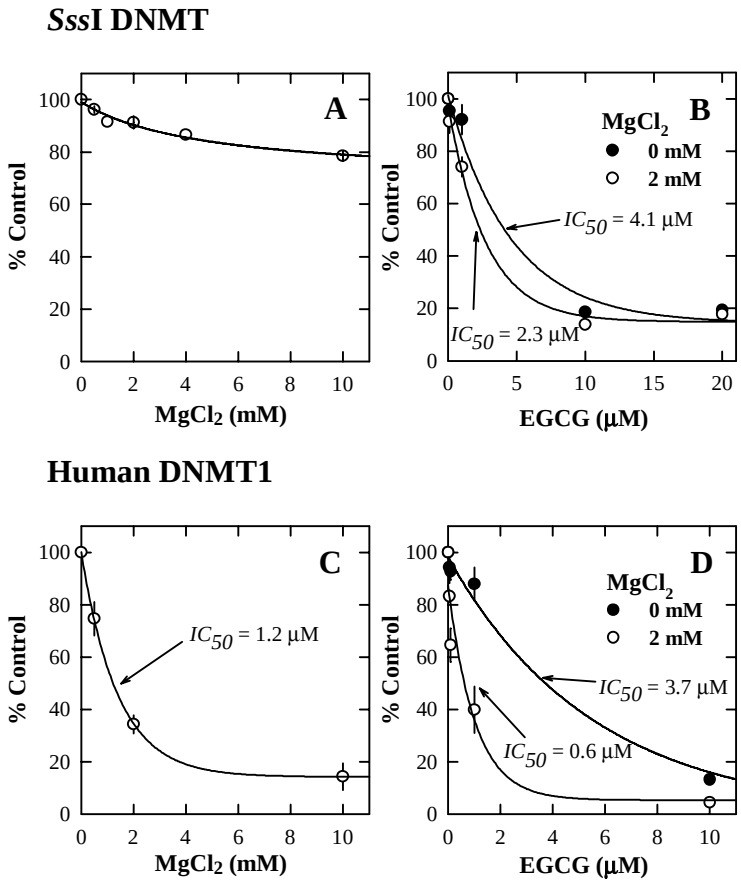

Fig. 8

Molecular Pharmacology Fast Forward. Published on July 21, 2005 as DOI: 10.1124/mol.104.008367
This article has not been copyedited and formatted. The final version may differ from this version.

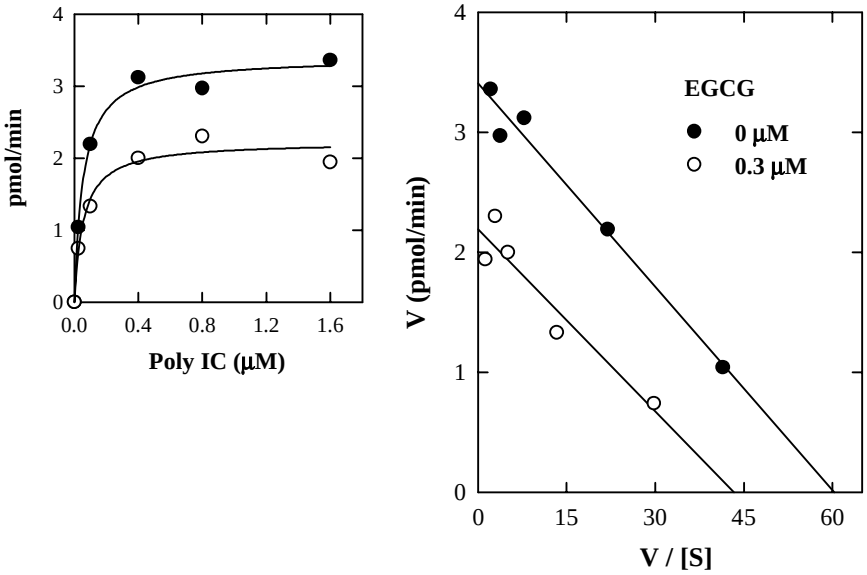

Fig. 9

Molecular Pharmacology Fast Forward. Published on July 21, 2005 as DOI: 10.1124/mol.104.008367
This article has not been copyedited and formatted. The final version may differ from this version.

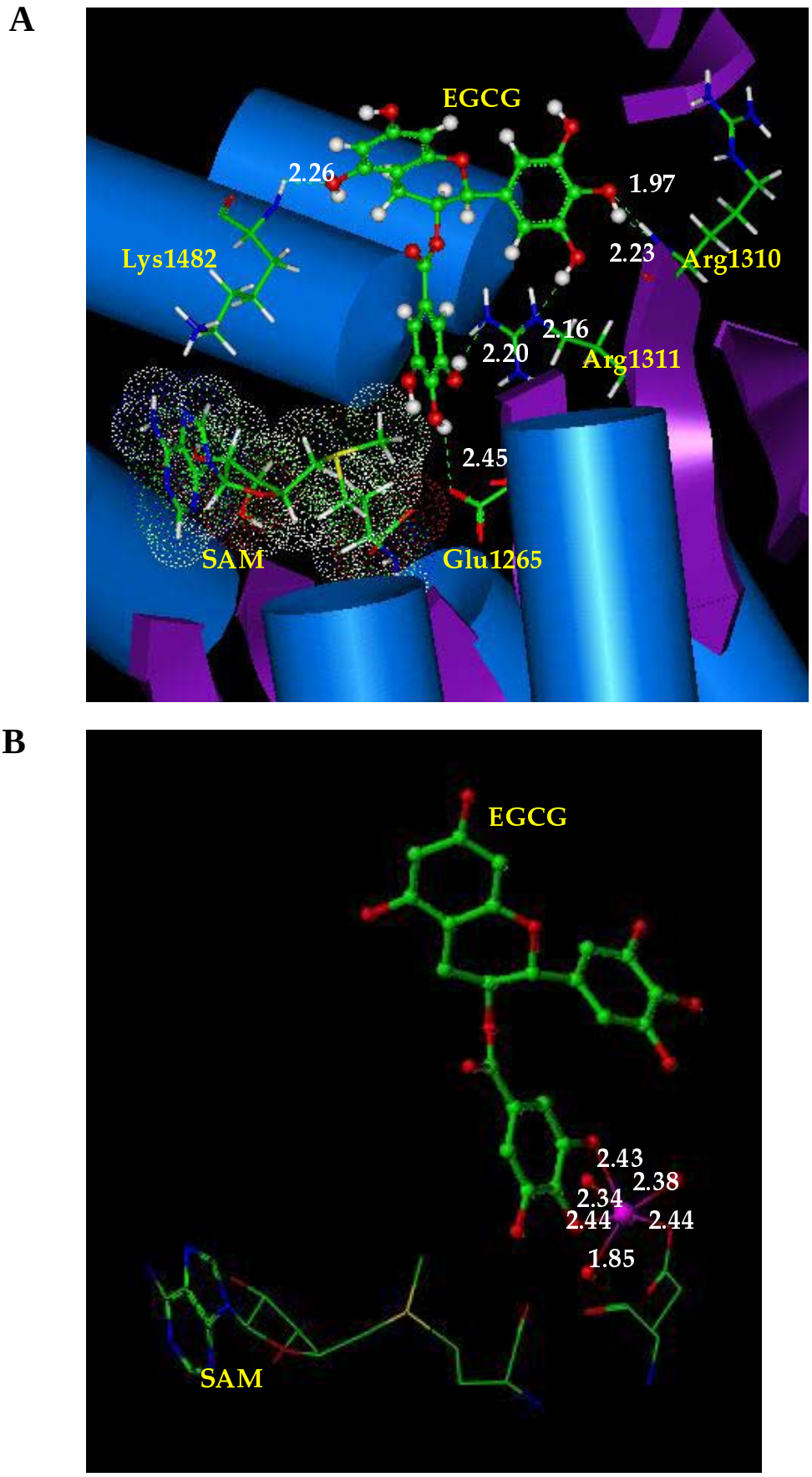

Fig. 10